

# SANDIA REPORT

SAND2011-6827  
Unlimited Release  
September 2011

## Anomaly Metrics to Differentiate Threat Sources From Benign Sources in Primary Vehicle Screening

Wondwosen Mengesha, Dov Cohen

Prepared by  
Sandia National Laboratories  
Albuquerque, New Mexico 87185 and Livermore, California 94550

Sandia National Laboratories is a multi-program laboratory managed and operated by Sandia Corporation, a wholly owned subsidiary of Lockheed Martin Corporation, for the U.S. Department of Energy's National Nuclear Security Administration under contract DE-AC04-94AL85000.

Approved for public release; further dissemination unlimited

Issued by Sandia National Laboratories, operated for the United States Department of Energy by Sandia Corporation.

**NOTICE:** This report was prepared as an account of work sponsored by an agency of the United States Government. Neither the United States Government, nor any agency thereof, nor any of their employees, nor any of their contractors, subcontractors, or their employees, make any warranty, express or implied, or assume any legal liability or responsibility for the accuracy, completeness, or usefulness of any information, apparatus, product, or process disclosed, or represent that its use would not infringe privately owned rights. Reference herein to any specific commercial product, process, or service by trade name, trademark, manufacturer, or otherwise, does not necessarily constitute or imply its endorsement, recommendation, or favoring by the United States Government, any agency thereof, or any of their contractors or subcontractors. The views and opinions expressed herein do not necessarily state or reflect those of the United States Government, any agency thereof, or any of their contractors.



SAND2011-6827  
Unlimited Release  
September 2001

# Anomaly Metrics to Differentiate Threat Sources From Benign Sources in Primary Vehicle Screening

Wondwosen Mengesha and Dov Cohen  
Radiation and Nuclear Detection System (8132)  
Sandia National Laboratories  
P.O. Box 969  
Livermore, CA 94551-0969

## Abstract

Discrimination of benign sources from threat sources at Port of Entries (POE) is of a great importance in efficient screening of cargo and vehicles using Radiation Portal Monitors (RPM). Currently RPM's ability to distinguish these radiological sources is seriously hampered by the energy resolution of the deployed RPMs. As naturally occurring radioactive materials (NORM) are ubiquitous in commerce, false alarms are problematic as they require additional resources in secondary inspection in addition to impacts on commerce. To increase the sensitivity of such detection systems without increasing false alarm rates, alarm metrics need to incorporate the ability to distinguish benign and threat sources. Principal component analysis (PCA) and clustering technique were implemented in the present study. Such techniques were investigated for their potential to lower false alarm rates and/or increase sensitivity to weaker threat sources without loss of specificity. Results of the investigation demonstrated improved sensitivity and specificity in discriminating benign sources from threat sources.

## **ACKNOWLEDGMENTS**

The Authors would like to acknowledge the support of the LDRD office of Sandia National Laboratories for funding the project. The Authors also acknowledge Isaac Shokair for the helpful discussions that were very crucial in writing this report.

# Contents

Acknowledgments.....	4
Figures.....	6
Tables.....	7
Nomenclature.....	8
1. Introduction.....	9
2 RPM Systems.....	12
2.1 PVT Detectors.....	12
2.2 Nuisance Alarm.....	13
2.3 Benign Sources.....	14
3.0 Data Mining.....	16
3.1. Principal Component Analysis.....	16
3.2. Cluster Analysis.....	16
3.3. Mahalanobis Distance.....	17
3.4. Data Fusion.....	17
4.0 GADRAS Simulation of RPM PVT Data.....	20
4.1 GADRAS Simulation Tool.....	20
5.0 Application of Anomaly Detection metric Using GADRAS Simulated DATA.....	26
5.1. Principal Component Transformation.....	26
5.2 Receiver Operating Characteristics (ROC) Curves.....	31
5.2.1 Performance in WGPu discrimination.....	32
5.2.2 Performance in RGPu discrimination.....	33
5.2.3 Performance in HEU discrimination.....	34
5.2.4 Performance in <sup>137</sup> CS discrimination.....	35
6 Clustering RPM data.....	37
6.1 Model based clustering.....	37
6.2 Clustering performance evaluation using ROC curves.....	38
7. Conclusions.....	39
8. References.....	40
Distribution.....	47

## FIGURES

Figure 1 Typical measured gamma spectrum from PVT for common commodity materials and background [4]. As can be seen in the spectra, there are no visible peaks that are from full energy absorption of incident gamma energy. ....	12
Figure 2 Simulated Th-232 PVT spectrum using GADRAS software [5]. As marked by differing colors, nine energy windows were established for spectral feature analysis. ....	13
Figure 3 GADRAS Modeling Framework. NYCT RPM data was simulated using empirical parameters recorded. Data was injected with known benign and threat gamma emitting radionuclides to assist in investigation of anomaly techniques. ....	20
Figure 4 Typical setup in GADRAS detector response function modeling. GADRAS uses layers of materials that represent the simulated detector and surrounding environment to implement particle transport. ....	21
Figure 5 Typical PVT gamma spectrum generated using GADRAS simulation tool. Counts detected as a result of gamma interaction were binned into 256 channels. The spectrum simulated is equivalent to one second detection time by the RPM modeled. ....	22
Figure 6 Grouped gamma counts from GADRAS simulation. Each spectrum simulated with 256 channels was regrouped into nine energy windows or channels to assist in anomaly detection techniques. The last energy window shows more spread due to poor statistics. ....	23
Figure 7 Principal Components evaluated for a selected benign source. As can be seen on the figure, the first principal component describes nearly 52% of the feature space. ....	27
Figure 8 Principal Components evaluated for background subtracted benign source. The second principal component has significantly changed and describes nearly 32% of the feature space..	27
Figure 9 Threat and benign source data mapped into PC feature space. Projections using the first three PCs show the most variability accounting noise and gamma scattering in low energy region. ....	28
Figure 10 Threat and benign source data mapped into PC feature space. Higher PCs, those above PC4, show a decreasing significance and variability. ....	29
Figure 11 Data projected back into pattern space from feature space using PC1 coefficients loading. The projected data shown in blue closely matches the original data. It is evident that PC1 reflects major characteristics features of the original curve. ....	30
Figure 12 Normalized mean value vector for individual energy windows used in the benign source data. The average counts reduce at higher energy regions. ....	30
Figure 13 Normalized standard deviation (sigma) vector for individual energy windows in the benign source data. ....	31
Figure 14 Calculated ROCs for Weapon Grade Plutonium (WGPu). Curves shown represent calculation based on projection of pattern space into feature space using varying PC components. MDs were then determined using the average of the benign source projections into the feature space. The orange line represents the non discriminating line. ....	32
Figure 15 Calculated ROCs for Reactor Grade Plutonium (RGPu). Curves shown represent calculation based on projection of pattern space into feature space using varying PC components. MDs were then determined using the average of the benign source projections into the feature space. The orange line represents the non discriminating line. ....	33
Figure 16 Calculated ROCs for Highly Enriched Uranium (HEU). Curves shown represent calculation based on projection of pattern space into feature space using varying PC components.	

MDs were then determined using the average of the benign source projections into the feature space. The orange line represents the non discriminating line. .... 34

Figure 17 Calculated ROCs for <sup>137</sup>Cs. Curves shown represent calculation based on projection of pattern space into feature space using varying PC components. MDs were then determined using the average of the benign projections into the feature space. The orange line represents the non discriminating line. .... 35

Figure 18 Plot of channel signals as a function of total signal counts. Discrete cluster groups are evident in the plot that deviates from linear trend. .... 37

Figure 19 Discriminant plot of clusters identified. .... 37

Figure 20 Calculated ROC curves for a threat source named V108. Curves shown represent calculation based on projection of pattern space into feature space using varying PC components basis. MDs were then determined using the average of the benign source projections into the feature space..... 38

Figure 21 Calculated ROCs for Very High Enriched Uranium (VHEU). .... 42

Figure 22 Calculated ROCs for <sup>90</sup>SrY. .... 43

Figure 23 Calculated ROCs for <sup>192</sup>Ir..... 44

Figure 24 Calculated ROCs for <sup>60</sup>Co. .... 45

## TABLES

Table 1 Source of interest in anomaly detection

## NOMENCLATURE

CBP	Customs and Border Protection
DU	Depleted Uranium
GADRAS	GAMMA Detector Response and Analysis
HEU	Highly Enrich Uranium
HPGe	High Purity Germanium (detector)
LEU	Low Enriched Uranium
N/FAP	Nuisance or False Alarm Probability
NORM	Naturally Occurring Radioactive Material
NYCT	New York Container Terminal
PNNL	Pacific Northwest National Laboratory
PCA	Principal Component Analysis
POE	Ports of Entry
PVT	Polyvinyl Toluene
RDD	Radiological Dispersal Device
RGPu	Reactor Grade Plutonium
RPM	Radiation Portal Monitor
SNL	Sandia National Laboratories
SNM	Special Nuclear Materials
WG Pu	Weapon Grade Plutonium



# 1. INTRODUCTION

U.S. Customs and Border Protection (CBP) has deployed Radiation portal monitors (RPMs) at ports of entries (POEs) and land crossing throughout the United States to monitor the trafficking of illicit radioactive materials. The RPM systems has also been deployed worldwide in many countries to inspect gamma and neutron emissions of vehicular and commercial traffic for the presence of special nuclear materials (SNM) and radioactive isotopes such as ones that can be used in radiological dispersal devices (RDDs). However, the presence of benign sources of radiation has been a problem and limits the effectiveness of discriminating such threat sources. Benign sources include naturally occurring radioactive materials (NORM) and isotopes used in medical treatments and industrial devices. These materials can trigger radiation alarms at POEs which require additional inspection and resources to assure security. Benign source caused alarms are commonly known as “nuisance” alarms and can have a significant impact on traffic flow, economy, and operations at POEs. Plastic scintillators and Helium gas detectors are the most widely used RPM detectors for gamma and neutron emission detection respectively and are used for screening cargo and vehicles at POEs and land crossings. Plastic scintillators are the cheapest gamma detectors that can be found in the market and explains the reason for their wide deployment. However due to their inherent poor energy resolution they lack the capacity for discriminating threat sources from benign sources based on resolved photo peaks. However their shortcomings in discriminating benign and threat source energies can be augmented by implementing advanced post data acquisition analysis. Techniques and analysis to distinguish benign and threat sources at POEs have been the subject of numerous studies. Runkle et al. [1] did investigation in RPM data analysis to enhance the sensitivity of detecting threat or anomaly sources using Principal Component Analysis (PCA). Their results were promising and indicate that there is a possibility of lowering Nuisance or False Alarm Probability (N/FAP) and increase sensitivity of RPM systems.

Anomaly sources or threat sources results in RPM measured signals from screening of cargo or vehicles that are unlikely related to expected patterns of benign source measurements. Anomaly or threat sources have signals that significantly differ from benign source population. Expected patterns are determined from analysis of historical data to estimate the distribution parameters such as means, variance, and modalities of the benign source population through the RPM system. These population distribution parameters are then used to establish anomaly detection thresholds that are more sensitive to weaker sources and are expected to achieve lower N/FAP. True alarms are decided through a statistical decision framework that implements a priori knowledge of benign source population or expected patterns to determine the likelihood of anomalous or threat signals.

The present project is aimed to investigate statistical techniques that can help lower the existing N/FAP and increase sensitivity of detecting threat sources at POEs. Based on such a framework, the following objectives have been the primary goals of the present investigation.

- To develop anomaly detection techniques to improve benign source discrimination in primary inspection at POEs. Therefore reduce nuisance alarm rates by increasing sensitivity to anomalies in the measured RPM data.

- To evaluate the performance of anomaly detection for sensitivity in anomaly detection
- Implement gamma and neutron sensors fusion to enhance the probability of detecting anomalous signals.
- To investigate and optimize energy window parameters to improve anomaly detection

To fulfill the project objectives simulated data based on the New York Container Terminal (NYCT) measurements were used to investigate techniques that may allow lowering the N/FAP. Sandia developed GAMMA Detector Response and Analysis (GADRAS) [2] particle transport software used in simulating background, benign, and threat source data. Using GADRAS generated data, Principal Component Analysis (PCA) and clustering techniques were implemented coupled to the Mahalanobis distance metric [3]. Receiver Operating Characteristic (ROC) curves were generated to highlight the performance and efficiency of the implemented techniques. Based on the investigation results, the implemented techniques show potential for lowering N/FAP at POEs. Further work, however, is required to refine and establish the techniques for the N/FAP reduction and efficient discrimination of benign sources from threat sources. However, fusion of gamma and neutron sensors has been found not to impact the project goals. Detection of a significant neutron signal above background is an outright indication of threat sources and it may not be necessary to go through implementation of statistical analysis that is described in the project. Therefore focus was made on scenarios that involve only gamma emissions either from benign or threat sources.

This page intentionally left blank

## 2 RPM SYSTEMS

### 2.1 PVT Detectors

Polyvinyl Toluene (PVT) is an organic plastic scintillator that is widely deployed in RPM systems for detecting gamma radiation emission in Cargo and vehicle screening at POEs. The wide implementation of PVT is mainly due to its relatively good sensitivity and cost-effectiveness compared to other detection materials. Pulse height or Gamma spectrum from PVT are broad distribution because gamma-rays interact primarily by Compton scattering with low atomic weight elements such as carbon and hydrogen. Typical measured gamma spectrum from PVT for common commodity materials and background are shown in Figure 1 [4]. The basic physics associated with PVT material hampers resolving the full energy deposition of gamma energy. PVT is therefore not used for discrimination of gamma energies and instead is used for gross counting of the gamma energy signals due to poor energy resolution. Gamma radiation interaction with PVT material results in the emission of light, which is detected by a photomultiplier tube (PMT) and converted into an electronic signal. This electronic signal is fed into an associated electronic circuit that counts the number of electronic signals from the PVT above a minimum set threshold energy. The Compton continuum observed in PVTs, however, contains some energy information that can be mined for discrimination of benign and threat sources at POEs using advanced techniques. The PVT gamma spectral response is binned into 256 channels. To facilitate the mining of information, thus the discrimination of benign and threat sources, the response is grouped under nine energy windows as shown in Figure 2 [5]. Each energy window represents the total sum of counts for a certain energy range. The number

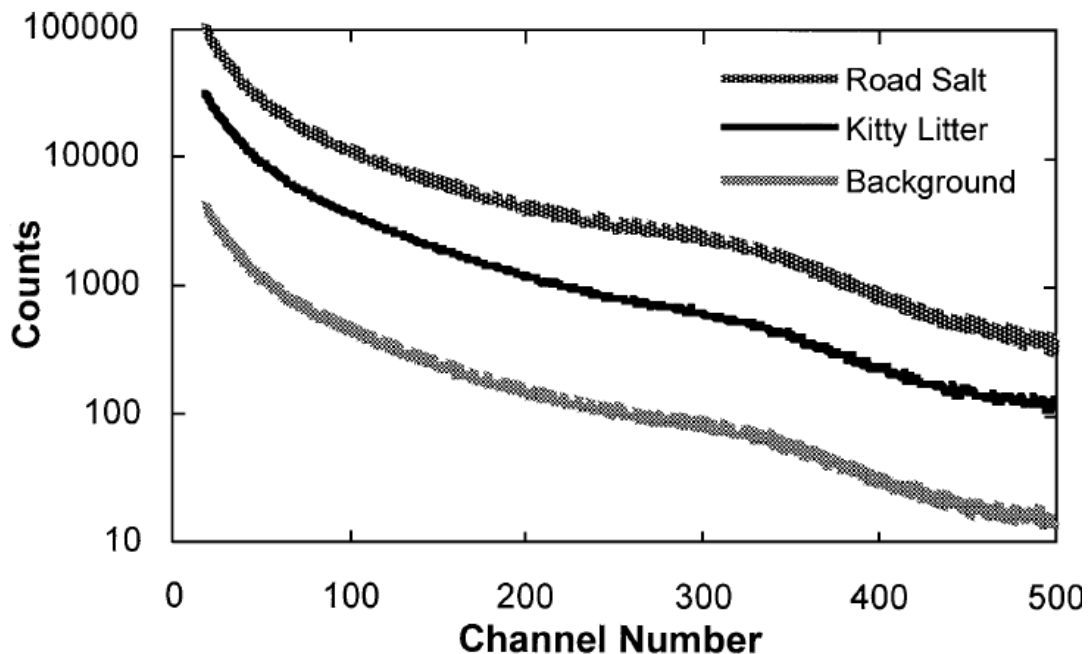


**Figure 1** Typical measured gamma spectrum from PVT for common commodity materials and background [4]. As can be seen in the spectra, there are no visible peaks that are from full energy absorption of incident gamma energy.

and width of the energy windows, however, is still a question of interest. Ely et al [4] discussed and tried to address this question in their work and have pointed out that proper energy windowing can help in discrimination of benign and threat sources through data mining.

## 2.2 Nuisance Alarm

RPMs deployed at the POEs commonly encounter alarms from statistical fluctuations in counts or from non-threat or benign sources. Gamma or neutron radiation can cause RPMs to trigger an alarm procedure. Alarms can be caused by statistical fluctuations of electronic signals registered by the RPM system. The alarm threshold set at POEs is fixed and any increased fluctuation above the threshold set can trigger the alarm (filtered signals are used for setting an alarm and therefore this type of alarm is not very common). These alarms are referred to as false alarms. Alarms can also be caused by benign sources loaded in cargos or vehicles. These alarms are referred to as nuisance alarms. Nuisance alarms have been a major concern since they result in disruption of traffic flow at the POEs and necessitate a secondary inspection. These alarms have significant impact on the economy, commerce, and demand for additional resources for screening alarming vehicle. It is also true that these alarms may not be associated with a single detector. In multi-lane architecture screening, several of these alarms may be triggered, which may be associated with a single cargo or vehicle with benign or possibly threat sources. In such cargo and vehicles screening scenarios, identifying the alarming vehicle is more difficult and possibly subject vehicles in the multi-lane screening system for a secondary inspection. It will not be difficult to figure out, in such cases, the impact on the traffic and

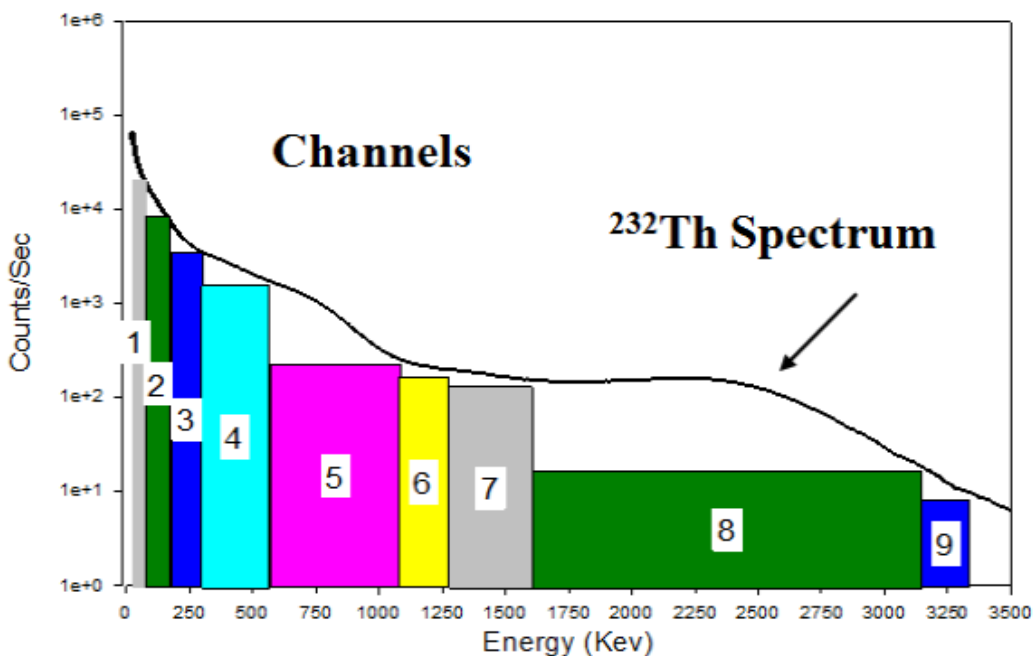


**Figure 2** Simulated Th-232 PVT spectrum using GADRAS software [5]. As marked by differing colors, nine energy windows were established for spectral feature analysis.

economy. Such nuisance alarms could have been avoidable, in principle, if better energy resolution detectors have been implemented at the POEs for discrimination of benign and threat sources. However, the multiple triggering scenarios, even though associated with poor energy resolution of the PVT in the RPM system, are beyond the scope of the present study. A single alarm caused by PVT RPM systems and the possibility of discriminating benign and threat sources and the possibility of enhancing sensitivity to threat sources is investigated.

## 2.3 Benign Sources

RPMs alarms are triggered by either Gamma radiation or neutron radiation. Alarms caused by statistical fluctuations that are intrinsic to radiation detection are referred to as false alarms. Alarms caused by benign radioactive sources that are ubiquitous are referred to as nuisance alarms. Nuisance alarms can be grouped into two major groups:

- 1 Naturally occurring radioactive materials (NORM) and technically enhanced NORM (TENORM)
  - a. Ceramic, tiles, porcelain, pottery, granite, clay, and other rock and clay based product contain elevated levels of naturally occurring  $^{40}\text{Potassium}$  and to a smaller degree  $^{232}\text{Thorium}$
  - b. Propane gas tankers, full or empty, contain elevated levels of  $^{226}\text{Radium}$
  - c. Many fertilizers and potash contain elevated levels of  $^{40}\text{Potassium}$
  - d. Cat litter contains elevated levels of  $^{232}\text{Thorium}$
- 2 Medical isotope alarms constitute the majority of alarms in privately owned vehicle lanes at land borders and are usually due to medical treatment of the driver or passengers, mostly due to  $^{99\text{m}}\text{Technetium}$   $^{201}\text{Thallium}$  and  $^{131}\text{Iodine}$ .

This page intentionally left blank

### 3.0 DATA MINING

Data Mining is a process of discovering new patterns from datasets using statistical analysis. It involves six distinct classes [6]:

- Anomaly detection also known as Outlier detection.
- Association learning that investigates relationship between variables
- Clustering that investigates groups having similar characteristics
- Classification involving categorizing data using known general structures
- Regression attempting to find a function modeling the data with minimized error
- Summarization representation of data set including visualization and report generation.

Pattern recognition techniques are effective tools that may be used to discover patterns and define boundaries in RPM data from cargo and vehicle screening at POEs. The basic idea in pattern recognition is to compare the input pattern with ones that are already stored in the memory and check for a match. Among the various pattern recognition techniques mentioned above, Principal Component Analysis (PCA) and Cluster Analysis techniques are used in the present study.

#### 3.1. Principal Component Analysis

Principal Component Analysis (PCA) is way of identifying patterns in data, and expressing the data in such a way so as to highlight their similarities and differences. Since patterns can be hard to find especially in high dimensional data, where the luxury of graphical representation is not available, PCA is a powerful tool for analyzing such data. The other main advantage of PCA is that once the patterns in the data are determined, the data can be compressed by reducing the number of dimensions, without much loss of information.

Assuming a data matrix  $X$ , there exists an image matrix  $Y$  that is determined using an orthogonal basis vectors given by  $V$ . Mathematically this may be expressed as:

$$Y = VX \quad (1)$$

PCA transforms the original variables  $X$  into new uncorrelated variables  $Y$ . The new variables are known as principal components. A metric for the amount of information conveyed by each principal component is its variance. Principal components are ordered in order of decreasing variance. Therefore the first principal component is the most informative in depicting the pattern in a dataset. Reduction in dimensionality or number of variables of the problem under investigation can be achieved by selecting the first few PCs without losing much of the information.  $X$  in the context of the present study represents data for the selected nine energy windows for a number of measurements. We may have as many rows as possible represented by the nine designated energy windows.  $Y$  is the original matrix  $X$  expressed by the new basis vectors defined orthogonally upon transformation. The new basis vectors are also known as feature vectors. Details on PCA techniques are given in [7].

#### 3.2. Cluster Analysis

Cluster analysis is a technique of assigning data into distinct groups, or clusters. Objects or data in the same cluster are more similar and related to each other than others in a different group or



cluster. Clustering algorithms group data based on a measure of similarity. Some examples of similarity metrics for quantitative data include: mathematical distance measure, absolute error between a monotonically increasing function, and a measure of correlation. Given a similarity measure, clustering algorithms group data points into clusters such that the within-cluster point scatter is minimized. Thus Cluster analysis is not a single process task. Instead it is an iterative process of knowledge discovery. In the present study a clustering technique known as MCLUST of the R code package [8] was used.

### 3.3. Mahalanobis Distance

The Mahalanobis distance is defined between two  $N$  dimensional points scaled by the statistical variation in each component of the point. Let  $x$  be a multivariable vector given as:

$$x = (x_1, x_2, \dots, x_n) \quad (2)$$

The mean of the multi dimensional vector is a single vector given by:

$$\bar{x} = (\bar{x}_1, \bar{x}_2, \dots, \bar{x}_n) \quad (3)$$

Using the covariance matrix  $COV$ , the Mahalanobis distance between the vector  $x$  and its mean is given by

$$D_M(x) = \sqrt{(x - \bar{x})^T COV^{-1} (x - \bar{x})} \quad (4)$$

The Mahalanobis distance is the same as the Euclidean distance if the covariance matrix is the identity matrix. It has the advantage of accounting for scaling of the coordinate axis. Additionally it accounts for correlation between the different features. Unlike the Euclidean distance, it provides curved as well as linear decision boundaries.

### 3.4. Data Fusion

Data Fusion is the use of techniques that integrate data from multiple groups or sources and unify the information gathered into decision making process that will be more efficient and accurate. Data fusion processes are commonly classified into low, intermediate or high, depending on the processing stage at which fusion takes place [9]. Low level fusion combines several sources of raw data to produce new raw data. The expectation is that fused data is more informative and synthetic than the original inputs. In the present project, data fusion was sought originally as a means of enhancing sensitivity and specificity in discrimination of benign and threat sources. Fusing neutron and gamma counts was one of the objectives of the present research to achieve the intended goal of effective discrimination of benign from threat sources. However, it was learnt in due process that, there is little that fusing of neutron and gamma counts add to the enhancement of sensitivity or specificity in anomaly detection. As it will be shown in section five, without even using the associated gamma counts, raised neutron counts by itself result in

almost 100% discrimination of benign from threat sources. Data Fusion of RPMs in multi-lane POEs, however, is of future interest that can be an effective solution in discriminating RPMs that trigger alarm in such scenarios.

This page intentionally left blank

## 4.0 GADRAS SIMULATION OF RPM PVT DATA

### 4.1 GADRAS Simulation Tool

GADRAS is a software application developed at Sandia National Laboratories (SNL) for gamma-ray spectral analysis for selected radiation detectors. GADRAS uses a full-spectrum analysis method to analyze gamma-ray spectra, where an entire spectrum is fit with one or more computed spectral templates [2]. GADRAS has the advantage in full spectral analysis of scintillators and semiconductor detectors such as HPGe. These templates are used to analyze gamma-ray spectra that are computed using a detector response function incorporated into GADRAS. Generation of parameter sets defining the detector response and characterization of empirical parameters that represent environmental scattering is also facilitated. This feature of GADRAS was utilized to enable generation of representative spectra from NYCT using benign and threat sources.

### 4.2 New York Container Terminal (NYCT) modeling

To help in the investigation of anomaly detection techniques, GADRAS was used to simulate RPM PVT Spectra representative of the NYCT data. The modeled dataset is based on empirical parameters recorded from the NYCT RPM system. Figure 3 shows the GADRAS modeling framework used in the present study.

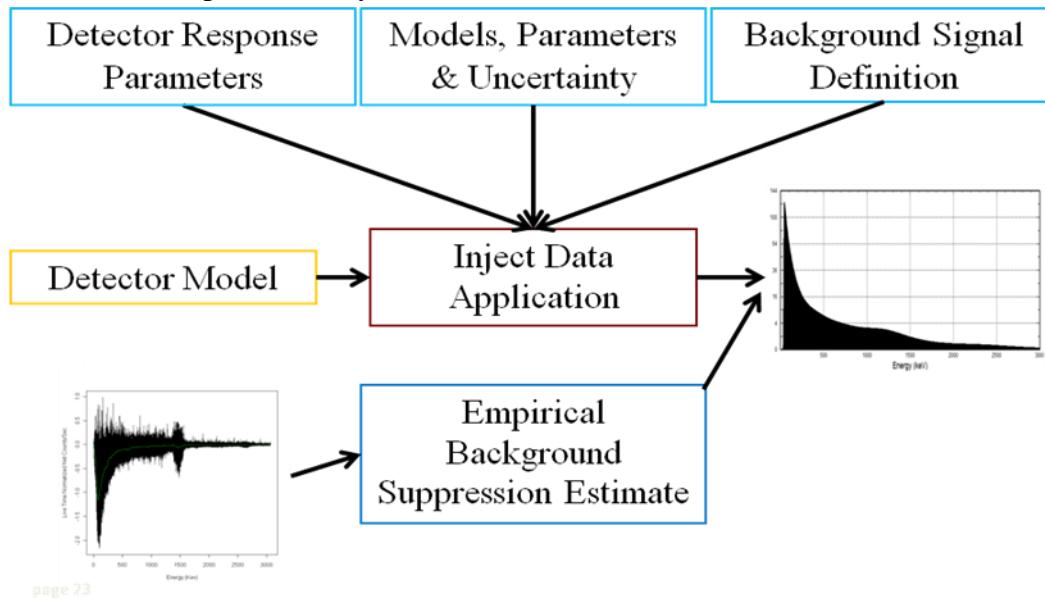


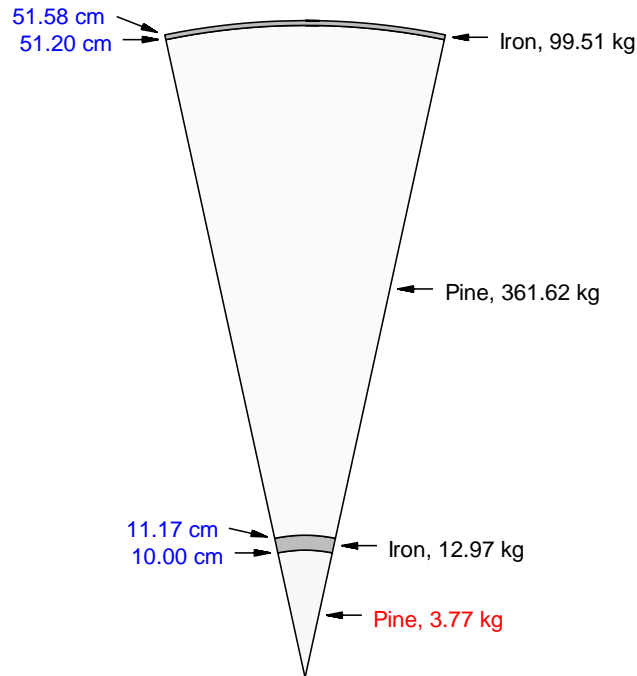
**Figure 3** GADRAS Modeling Framework. NYCT RPM data was simulated using empirical parameters recorded. Data was injected with known benign and threat gamma emitting radionuclides to assist in investigation of anomaly techniques.

Based on empirical source parameters and detector response parameters of the NYCT RPM detector deployed, simulation of background, benign, and threat source modeling was done using GADRAS. It is a known fact that during the screening process of a cargo or a vehicle that background suppression results from shielding of the background by the moving vehicle structure and cargo. Estimated background suppression was integrated in the simulation.

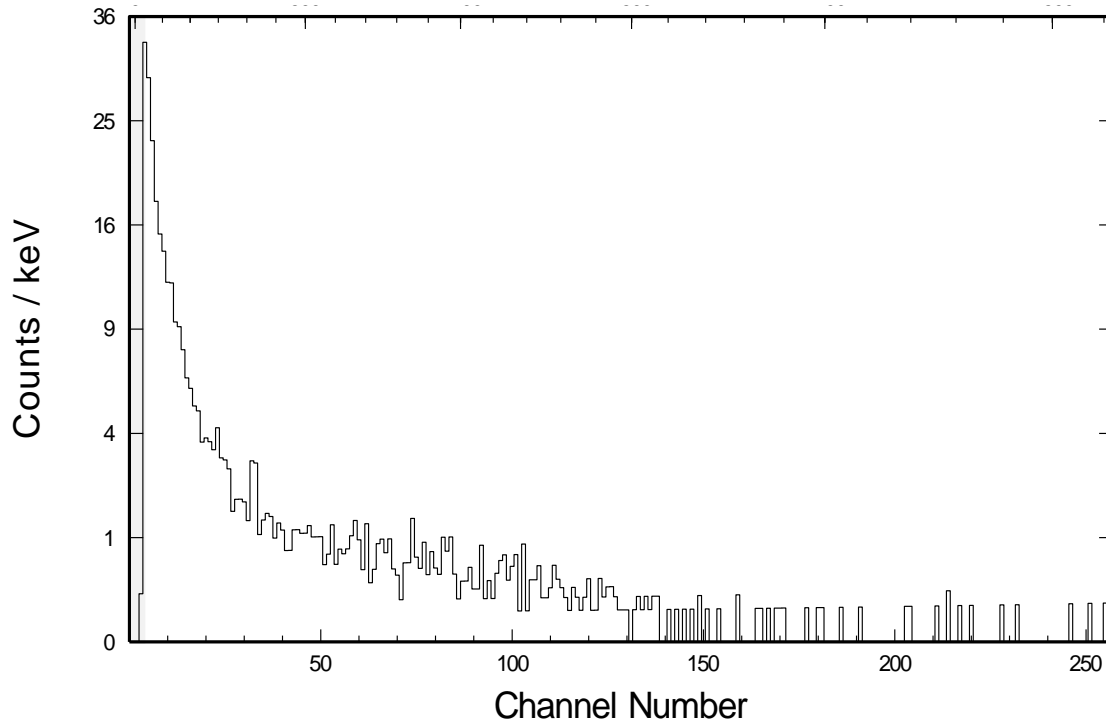
Injection was then made of known benign and threat isotopes at different activity levels. Some known sources of interest are shown in Table 1. Typical setup in the GADRAS simulation of detector response function is shown in Figure 4.

Table 1  
Sources of interest in anomaly detection

<b>SNM and Uranium</b>	<b>Industrial</b>	<b>Medical</b>
WG Pu	$^{60}\text{Co}$	$^{133}\text{Ba}$
RGPu	$^{137}\text{Cs}$	$^{99\text{m}}\text{Tc}$
HEU	$^{90}\text{Sr}$	$^{201}\text{Tl}$
LEU		$^{131}\text{I}$
DU		$^{192}\text{Ir}$
$^{237}\text{Np}$		
$^{232}\text{U}$		
Natural Uranium		



**Figure 4** Typical setup in GADRAS detector response function modeling. GADRAS uses layers of materials that represent the simulated detector and surrounding environment to implement particle transport.



**Figure 5** Typical PVT gamma spectrum generated using GADRAS simulation tool. Counts detected as a result of gamma interaction were binned into 256 channels. The spectrum simulated is equivalent to one second detection time by the RPM modeled.

A total of 256 channels were used to bin detected counts from gamma transport through the simulated medium. A one second equivalent detection time was used in the simulation. Figure 5 shows a representative spectrum for one of the threat sources modeled based on the NYCT response parameters.

Figure 5 shows a continuum of counts detected as a result of gamma interactions in the detector medium. There are no distinct peaks to allow spectroscopic analysis for the reason of poor energy resolution in PVT detectors. Poor statistics due to the short one second detection time might also make photo peak detection difficult for higher resolution scintillation or semiconductor detectors. In principle one can do pattern recognition using PCA or cluster analysis straight with this simulated spectrum. However, this requires the definition of 256 dimensions or variables that will make calculation and analysis very complex and complicated. Therefore as it is discussed by Ely et al., energy windowing or grouping is the best option to avoid the cumbersomeness in the implementation of anomaly detection techniques. Apart from simplifying the calculation process, energy windowing has also the advantage of increasing the signal-to-noise ratio for statistically improved data analysis. As shown in Figure 2, simulated spectra were grouped into nine energy windows or channels to assist the analysis. Accordingly all counts in channels allocated to a given window or channel are summed to give one data point or dimension in the anomaly technique implementation. Therefore nine counts or dimensions represent a vector for a single measurement. Energy windows implemented by Pacific Northwest National Laboratory (PNNL) was assumed in the present analysis. Figure 6 shows the plot for the nine energy windows regrouped for the benign source population. As can be seen in the

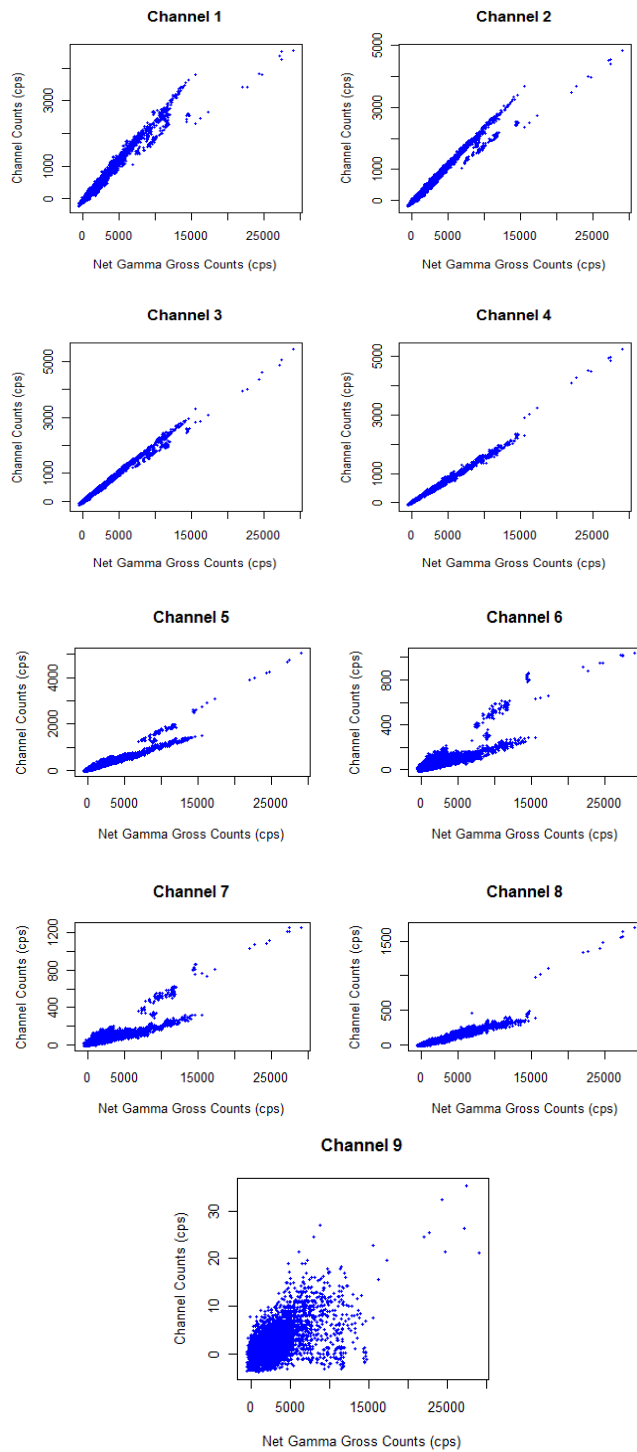


**Figure 6** Grouped gamma counts from GADRAS simulation. Each spectrum simulated with 256 channels was regrouped into nine energy windows or channels to assist in anomaly detection techniques. The last energy window shows more spread due to poor statistics.

figure, variations in individual channel counts per second are evident as a function of the total counts per second. Both counts on the abscissa and the ordinate are background subtracted and represent net counts. Depending on the injected source type and its energy significance in the corresponding channels, departures from a linear trend line is observed in the plots. The energy ranges for the nine windows and associated channels are shown in Figure 2.



This page intentionally left blank

## 5.0 APPLICATION OF ANOMALY DETECTION METRIC USING GADRAS SIMULATED DATA

### 5.1. Principal Component Transformation

Data simulated using the GADRAS software was used for PCA in the present study. The data as described in previous section is configured using parameters from the NYCT RPM measurements. Results from typical benign source data PCA analysis are shown in Figure 7. To make the PCA analysis made clear, two domains or spaces are adopted that are associated to the modeled data before and after PCA transformation. Accordingly, the original data before transformation is understood to be in the original or pattern space/domain and after its transformation it is understood to be in PC or feature space/domain. As can be seen from the figure, the first principal component, also known as the first eigen value, describes nearly 52% of the observed feature space. The remaining 48% feature space is described by the remaining PC components. It is expected that significant variation in the simulated spectrum is due to the low energy region that is also characterized by noise and scattered gamma rays. Subtracting the background data from each data representing a one second counts gives the net count mainly from the benign source injection made in the background. Carrying out the PCA analysis on the net counts gives results shown in Figure 8. The result shows similar percentage of the first principal component. Increase in the second component is evident after the background subtraction. In this particular case the first three PCs that account ~96% of the feature space may be sufficient to characterize the spectra. This allows the reduction of the dimension from nine to three. Similar to the spectrum with background data included, the background subtracted spectrum has significant variation around the low energy area, where the energy region is dominated by gamma scattering.

Figure 9 shows plots of the original normalized threat and benign source data projected into PC space. It is evident from the plots that projecting the normalized data using the first three PCs shows the most variability in the feature space. Higher PCs show a decreasing significance and variability as can be seen in Figure 10. Therefore it may be sufficient to use the first three PCs, for the sources simulated, for effective discrimination of benign from threat sources. Figure 10 shows back projection of the benign data into the original pattern space. The red line represents the original data. The blue line represents back projection of the data using PC1 from feature space back to the pattern space. As it is evident, PC1 reflects major characteristics features of the original curve. This makes sure that PCA analysis is working as expected. The basis vectors or Eigen vectors generated from PCA analysis were used to project the original data into feature space and back from feature space into pattern space. Figure 11 and 12 represents the normalized mean and standard deviation for the benign source population considered.

Identification of outliers as shown in Figure 6 is achieved by implementing appropriate metric suitable for discrimination. The Mahalanobis distance (MD) described in the previous section was used to effectively discriminate benign source population from threat sources by computing the distance from the expected average of the benign population in the feature space. The MD was calculated using equation 4 in section 3. The original or pattern data had to be mapped into feature space before the MD calculation. It is described in section 3 that using more PCs may

describe subtle or more features of the pattern or original space. At the same time redundant features may be included. After the MD calculation the Receiver Operating Characteristics (ROC) was calculated using an MD threshold associated with a specific false alarm Rate (FAR).

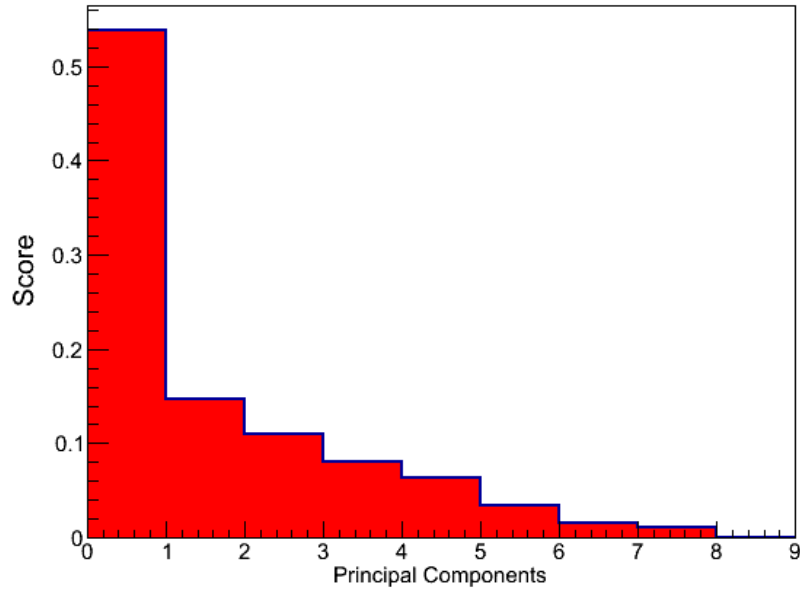


**Figure 7** Principal Components evaluated for a selected benign source. As can be seen on the figure, the first principal component describes nearly 52% of the feature space.

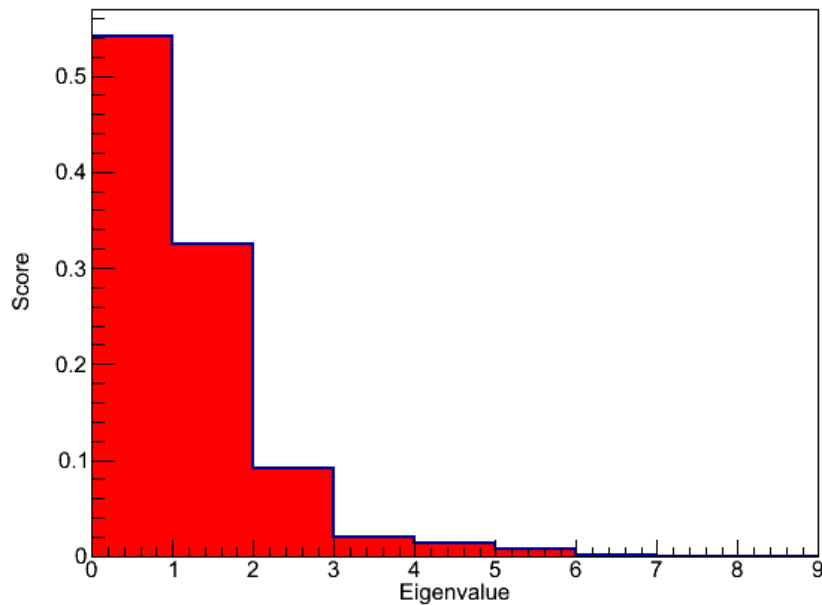


**Figure 8** Principal Components evaluated for background subtracted benign source. The second principal component has significantly changed and describes nearly 32% of the feature space.

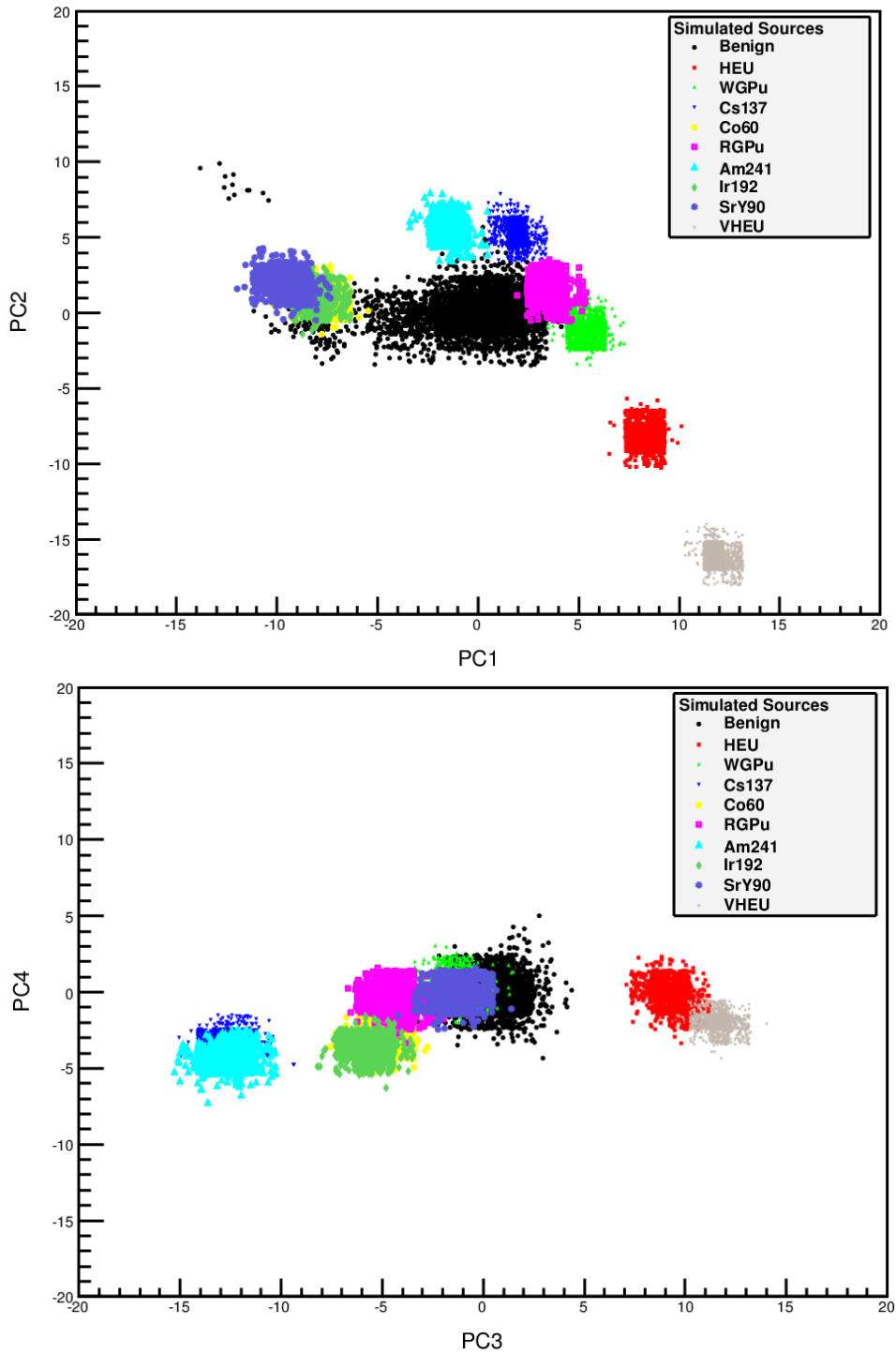


**Figure 9** Threat and benign source data mapped into PC feature space. Projections using the first three PCs show the most variability accounting noise and gamma scattering in low energy region.

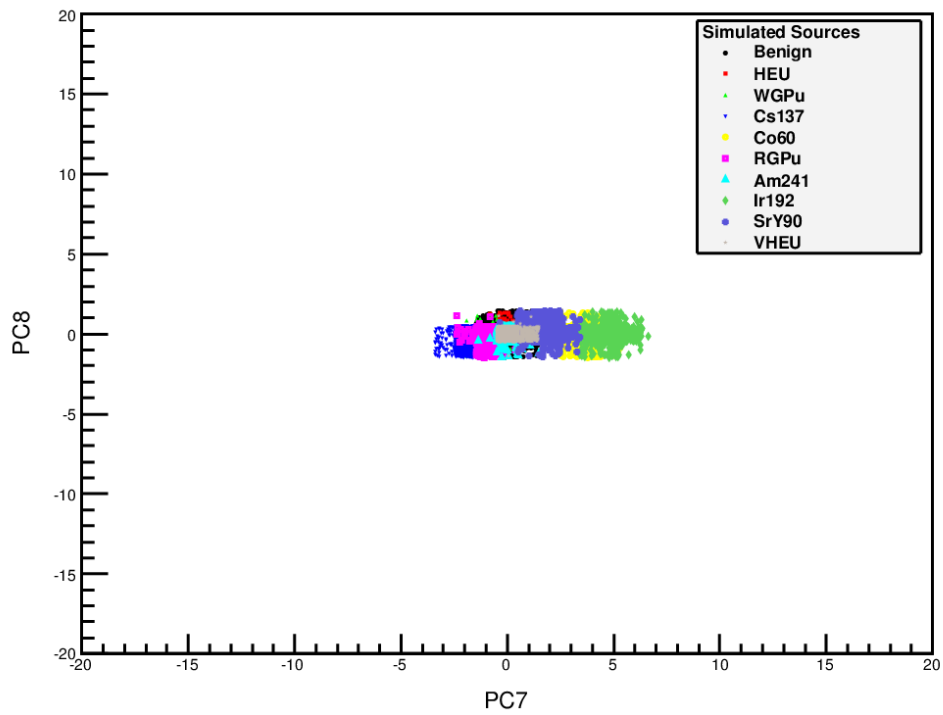
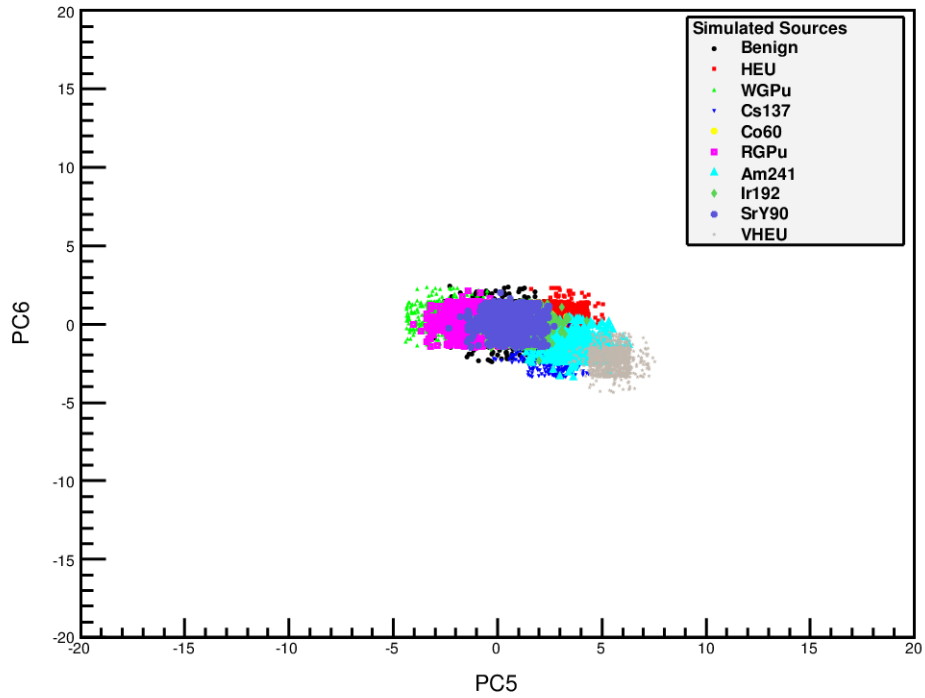


**Figure 10** Threat and benign source data mapped into PC feature space. Higher PCs, those above PC4, show a decreasing significance and variability.

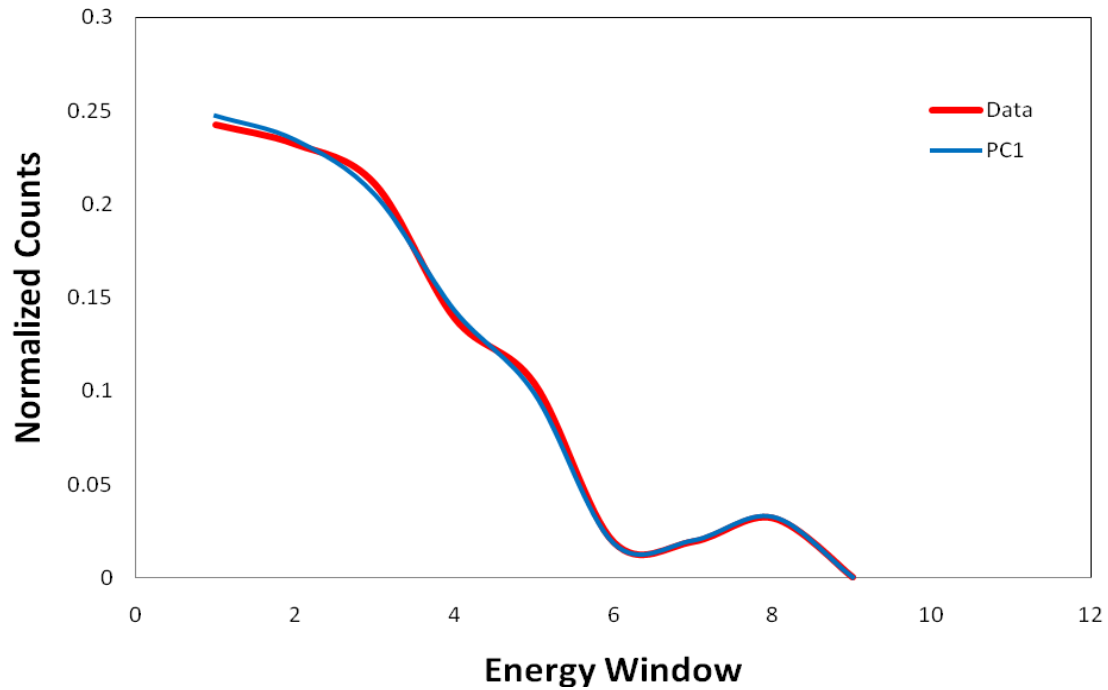


**Figure 11** Data projected back into pattern space from feature space using PC1 coefficients loading. The projected data shown in blue closely matches the original data. It is evident that PC1 reflects major characteristics features of the original curve.

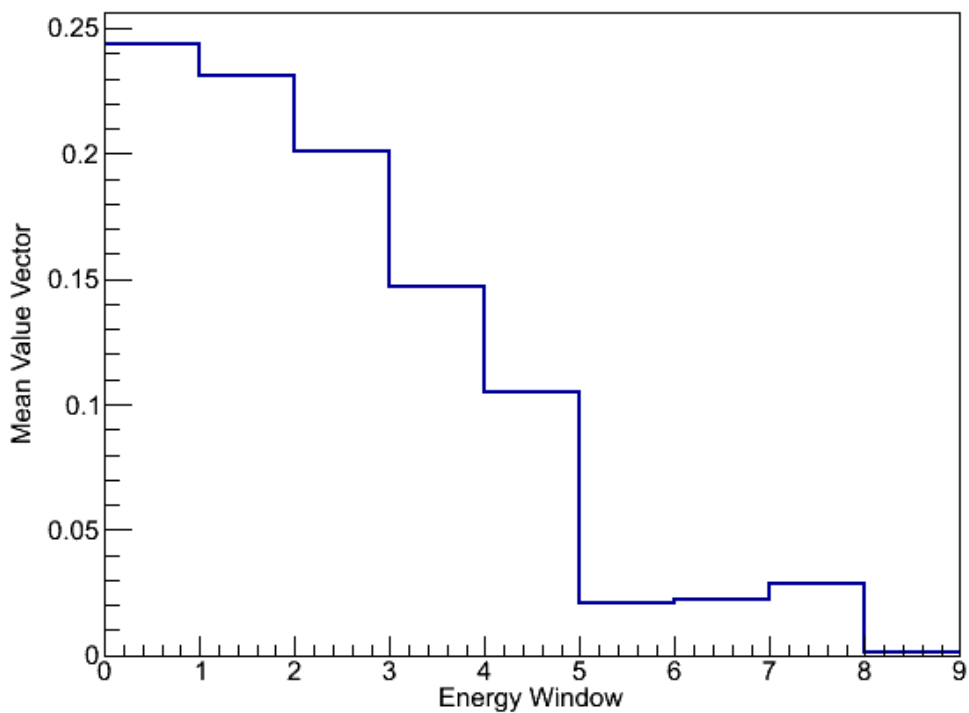


**Figure 12** Normalized mean value vector for individual energy windows used in the benign source data. The average counts reduce at higher energy regions.

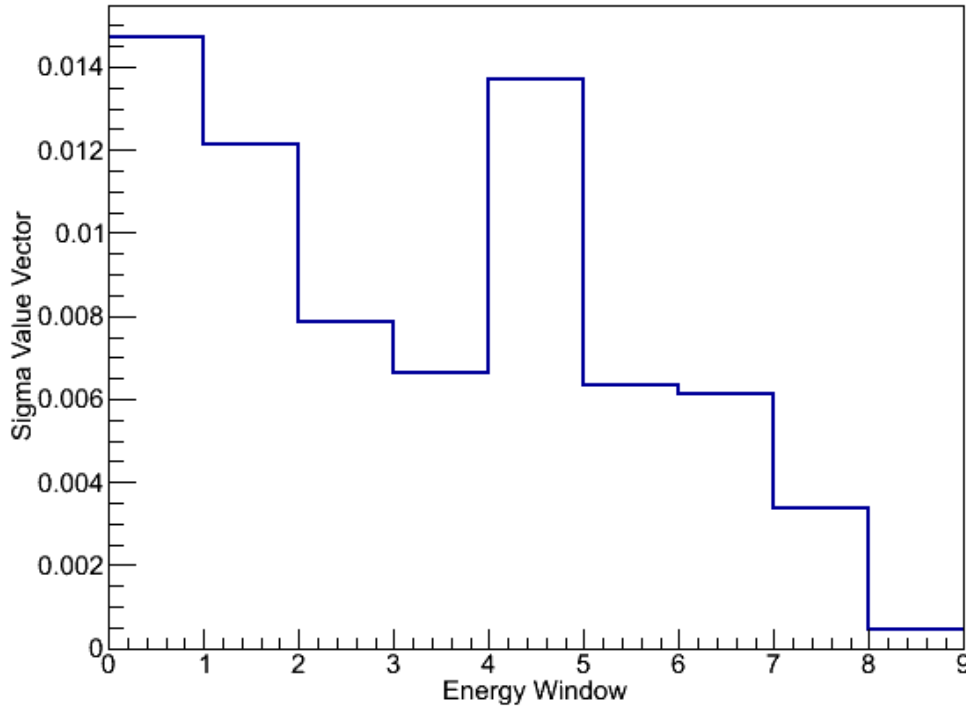


**Figure 13** Normalized standard deviation (sigma) vector for individual energy windows in the benign source data.

## 5.2 Receiver Operating Characteristics (ROC) Curves

ROC curves enable evaluation of sensitivity and specificity of an employed detection technique and are fundamental tools for diagnostic test evaluation. In the present study, ROC curves demonstrate if the statistical techniques implemented are more sensitive and specific in discrimination of benign from threat sources compared to traditional way using gross counts for discrimination.

In a ROC curve the true positive rate (Sensitivity) is plotted as a function of the false positive rate (Specificity) for different cut-off points of a parameter. The cut-off points in the present context are determined by the MD limits. Each point on the ROC curve represents a sensitivity-specificity pair corresponding to a particular decision threshold. The area under the ROC curve (AUC) is a measure of how well a parameter can distinguish between two diagnostic groups.

ROC curves were generated for the threat sources produced using GADRAS injection modeling. The purpose of the ROC curves is to demonstrate how well the technique implemented can discriminate the benign source population from the threat source population. ROC curves generated were for threat radio-nuclides listed in Table 1 using a range of FAR.

### 5.2.1 Performance in WGPu discrimination

Figure 13 shows the ROC curves produced using the WGPu injected source. The curves shown represent calculations based on projection of the normalized counts into feature space using varying PC components. MDs were then determined using the average of the benign source projections into the feature space. The orange line represents the non discriminating line or where there is no advantage gained in indiscriminating benign from threat sources. ROC curves for gross counts and neutron counts were determined using the traditional way of setting thresholds using summed or total counts. As can be seen on the curves for false alarm rate below ~0.25, the technique is doing worse, as all curves are below the discrimination line.

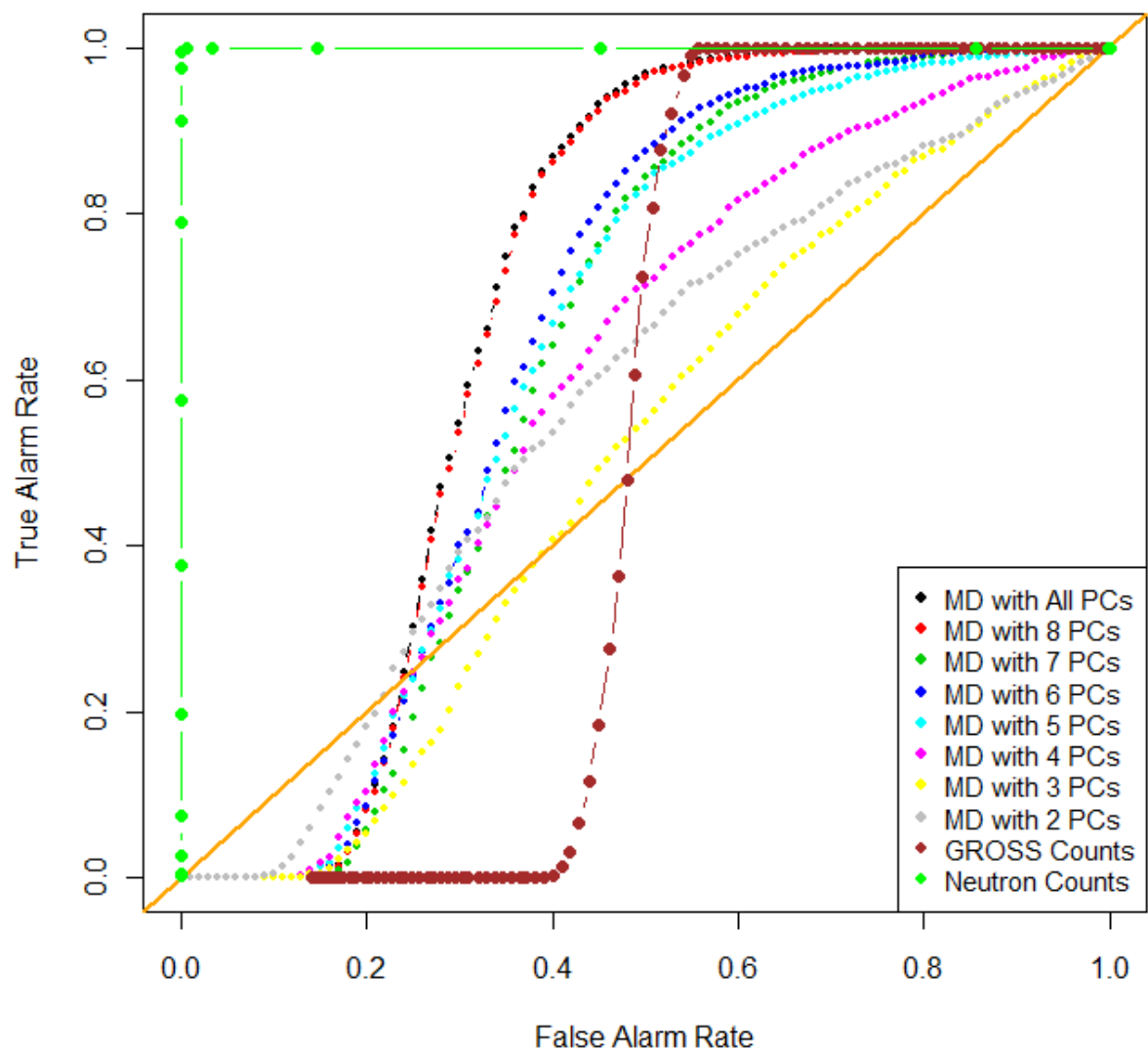


**Figure 14** Calculated ROCs for Weapon Grade Plutonium (WGPu). Curves shown represent calculation based on projection of pattern space into feature space using varying PC components. MDs were then determined using the average of the benign source projections into the feature space. The orange line represents the non discriminating line.



However, for the neutron counts the technique shows ideal performance due to high neutron flux above the neutron background that will be easy for discrimination WGPU from a benign source population using the traditional gross counts approach. In general the more PCs are included in projecting the pattern into feature space, the better is the performance, but this is not true for all cases. Some discrepancy is evident in the graph. MD calculated using 6 PCs and 7 PCs shows the reverse of expected results. Better performance is expected in using 7 PCs than 6 PCs. Same is true with MD from 3 and 2 PCs. More detail investigation is required to understand these results. The results in Figure 13 shows that the PCA anomaly detection technique has advantages over using gross gamma counts, within the window of FAR values in the range  $\sim 0.225$  to  $0.45$ .

### 5.2.2 Performance in RGPU discrimination

The results for RGPU, shown in Figure 14, demonstrate better discrimination than WGPU for the MDs considered. Although not ideal like the WGPU case, the neutron counts are clear outliers and can easily be discriminated using the traditional gross counts approach. The same discrepancy observed in WGPU in terms of the number of PCs used is also evident in the RGPU case requiring attention in future work.

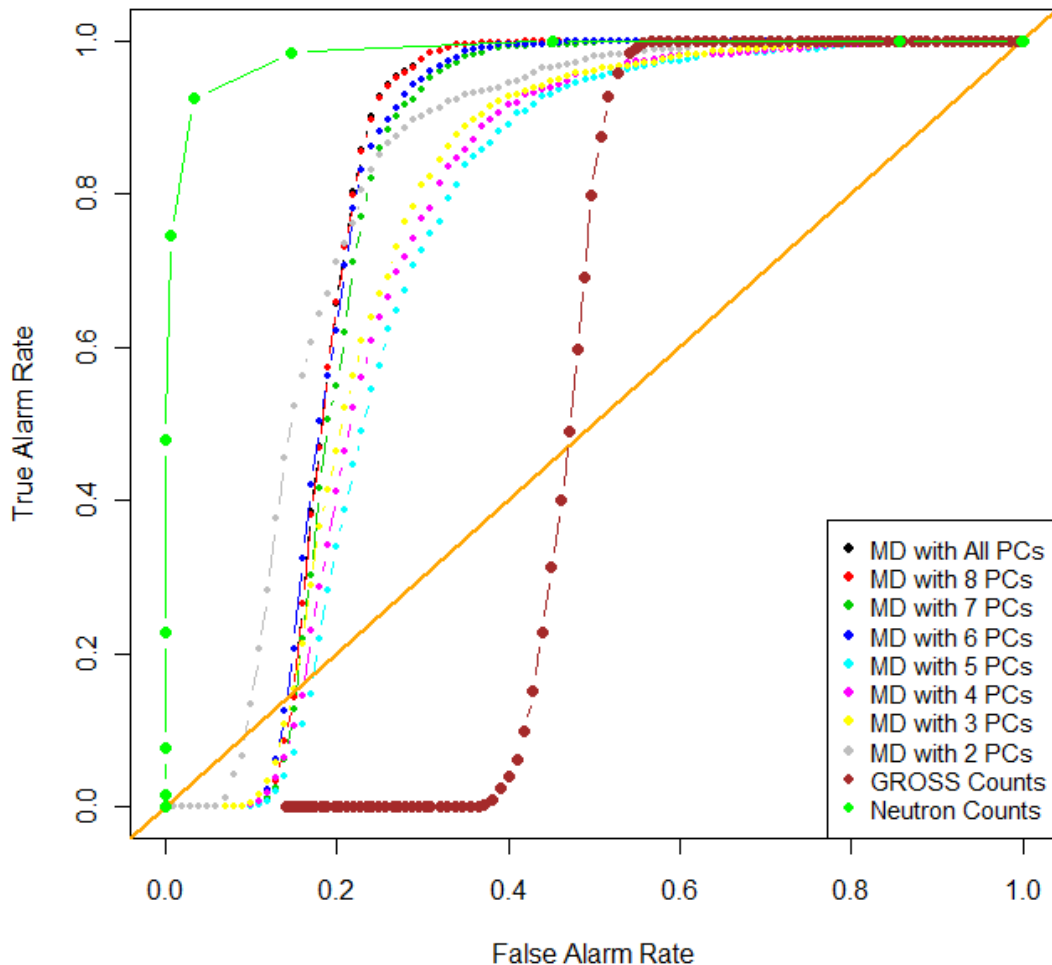


**Figure 15** Calculated ROCs for Reactor Grade Plutonium (RGPU). Curves shown represent calculation based on projection of pattern space into feature space using varying PC components. MDs were then determined using the average of the benign source projections into the feature space. The orange line represents the non discriminating line.

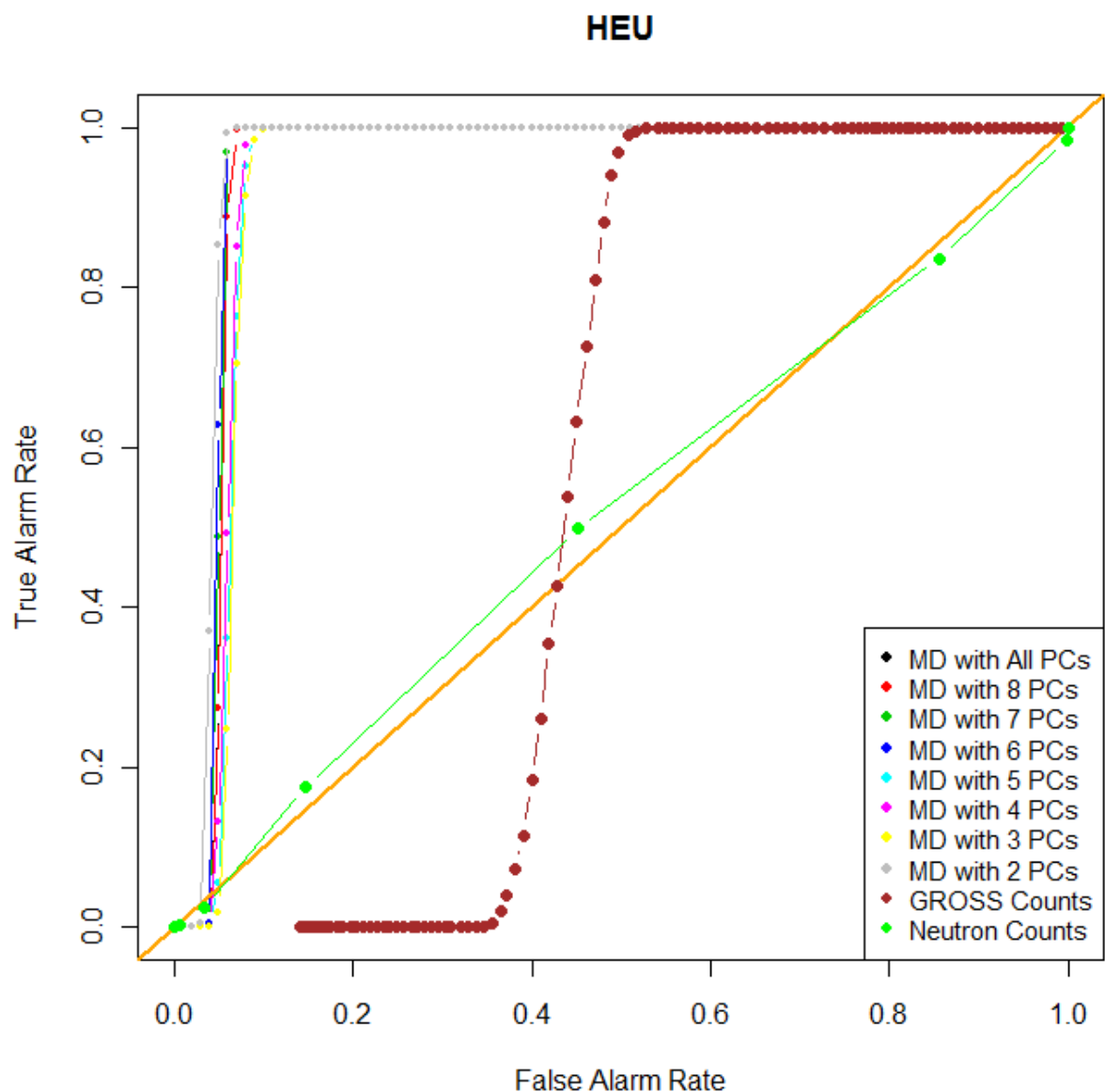


**Figure 16** Calculated ROCs for Highly Enriched Uranium (HEU). Curves shown represent calculation based on projection of pattern space into feature space using varying PC components. MDs were then determined using the average of the benign source projections into the feature space. The orange line represents the non discriminating line.

### 5.2.3 Performance in HEU discrimination

The HEU performance, shown in Figure 15, is almost ideal with respect to sensitivity or specificity. The PCA technique can easily discriminate the HEU outlier at very low FAR. However, there is hardly any discrimination using gross neutron counts using the traditional approach.

#### 5.2.4 Performance in $^{137}\text{CS}$ discrimination

The  $^{137}\text{CS}$  performance, shown in Figure 16, is also almost ideal with respect to sensitivity or specificity. The PCA technique can easily discriminate the  $^{137}\text{CS}$  at very low FAR better than gross counts threshold. More ROC curves produced for other isotopes are shown in Appendix A.

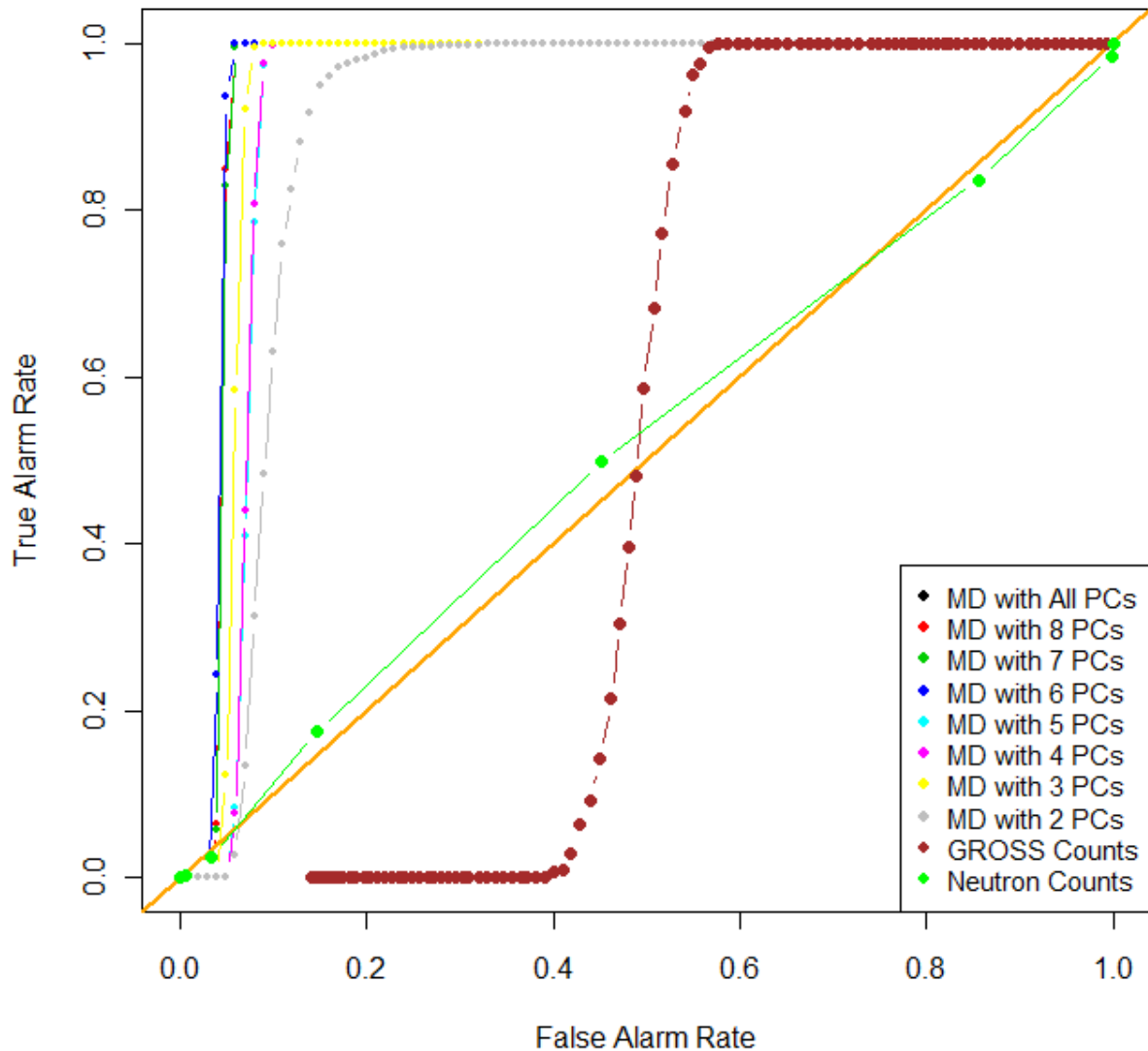


**Figure 17** Calculated ROCs for  $^{137}\text{Cs}$ . Curves shown represent calculation based on projection of pattern space into feature space using varying PC components. MDs were then determined using the average of the benign projections into the feature space. The orange line represents the non discriminating line.

This page intentionally left blank

## 6 CLUSTERING RPM DATA

### 6.1 Model based clustering

An R software package MCLUST was used for the clustering. The package is for normal mixture and model based clustering. MCLUST provides functions for parameter estimation via Expectation Maximization (EM) algorithm for normal mixture models with a variety of covariance structures, and functions for simulation from these models. Pattern data was first transformed into PC space before clustering. Different set of data was used in the Cluster Analysis. The Analysis was made prior to using NYCT simulated data. Therefore direct comparison with the NYCT data is not possible. A threat source named V108 was used in the clustering technique. Clusters in the present study were identified using the Gaussian mixture clustering algorithm. Figure 17 shows a linear plot of channel signals as a function of total signals for the different MCLUST clustered groups. Discriminant plot of the clusters identified is shown in Figure 18.

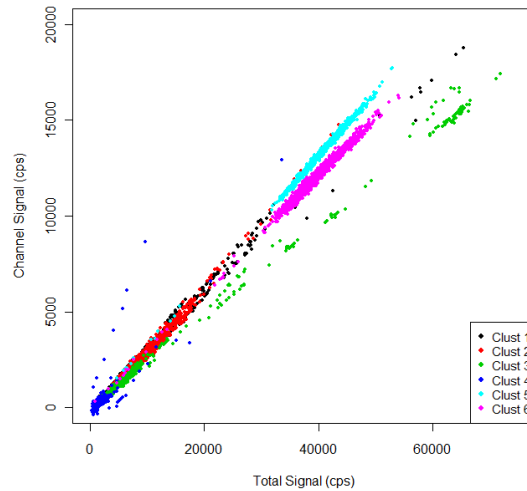


**Figure 18** Plot of channel signals as a function of total signal counts. Discrete cluster groups are evident in the plot that deviates from linear trend.

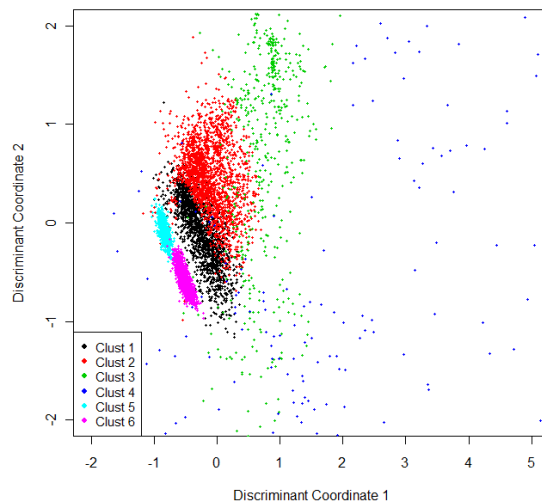


**Figure 19** Discriminant plot of clusters identified.

## 6.2 Clustering performance evaluation using ROC curves

Similar to PCA analysis the Mahalanobis distance for anomaly discrimination was calculated after feature space transformation. Distances were calculated from the average of the clusters distribution. ROC curves were then used to assess the performance of the clustering technique, in the same way done for the previous PCA analysis.

Similar to PCA analysis, the clustering technique also proved improvement in detection performance compared to gross counts as shown in Figure 19. Separate plots are made for true alarm rate as a function of FAR based on the MD calculated using a range of PCs.

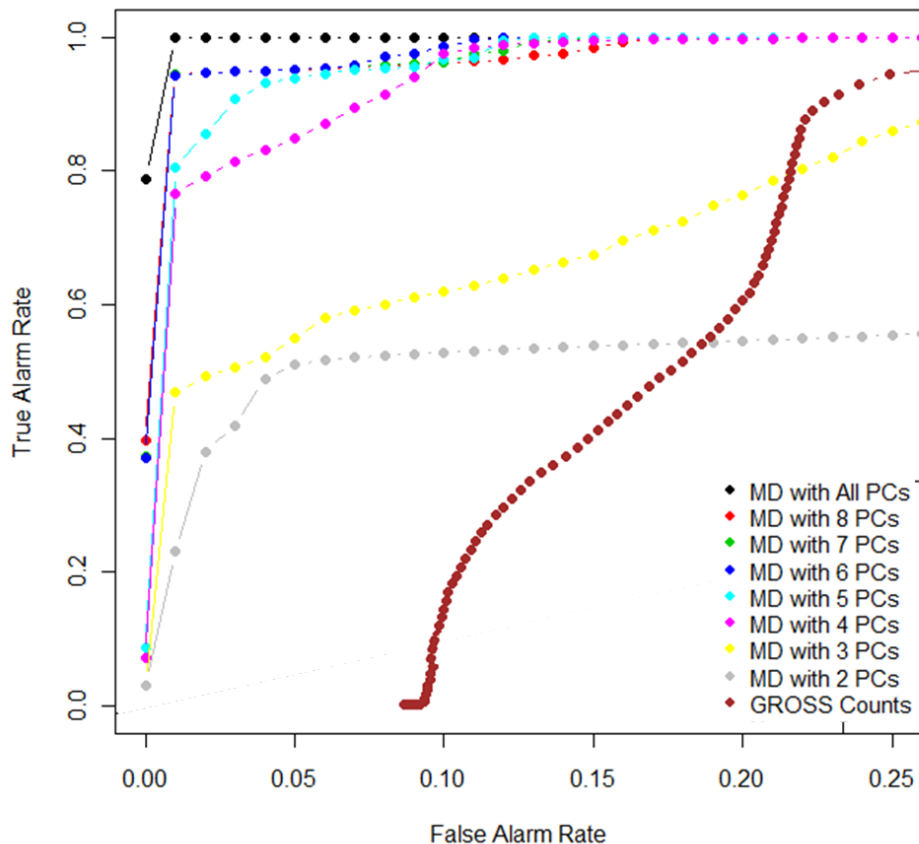


**Figure 20** Calculated ROC curves for a threat source named V108. Curves shown represent calculation based on projection of pattern space into feature space using varying PC components basis. MDs were then determined using the average of the benign source projections into the feature space.

## 7. CONCLUSIONS

Anomaly detection techniques implemented in the present study showed improvements in sensitivity and specificity of discriminating benign source population from threat source population compared to the traditional gross counts approach. Encouraging results have been found in the performance of the techniques. The PCA technique coupled with clustering can be beneficial in defining optimal and minimized thresholds for alarming at POEs. This, however, was not confirmed since the same of data set was not used for PCA only and PCA with clustering technique implemented. This will be investigated in detail in future work. The present work was not able to investigate optimization of energy windows used in the analysis. It is believed that based on the physics of gamma interaction with the RPMs and iterative maximization of feature variances in PC space by varying energy windows, further enhancement and improvement can be achieved in anomaly discrimination. Data used in the analysis represent static and simulated data. It is not characterized by temporal features and other uncertainties related to actual measured data. These may include gain variation in the RPM detectors, electronic noise, and other systematic errors that can cause significant deviation from Poisson statistics. Implementation of investigated techniques using measured data is required to address these issues.

Data fusion was not implemented for enhancement of sensitivity using neutron and gamma information. It has been found that fusion of neutron and gamma data will not have an impact on sensitivity enhancement as the neutron data alone will enable the discrimination of benign sources from threat sources. This fact is obvious in ROC curves produced in section 5.

## 8. REFERENCES

- 1 R.C. Runkle, M.F. Tardiff, K.K Anderson, D.K. Carlson, and L.E. Smith, *Analysis of Spectroscopic Radiation Portal Monitor Data Using Principal Component Analysis*, IEEE Trans. Nucl. Sci. Vol. 53, No. 3, pp. 1418-1423, June 2006.
- 2 *Gamma Detector Response and Analysis Software (GADRAS)*, Dean J. Mitchell, Sandia National Laboratories, 1986.
- 3 P.C. Mahalanobis, *On the Generalized Distance in Statistics*, The National Institute of Sciences of India, Vol. II, No. 1, pp. 49-55, 1936.
- 4 J.H. Ely, R.T. Kouzes, B.D. Geelhood, J.E. Schweppe, and R.A. Warner, *Discrimination of Naturally Occurring Radioactive Material in Plastic Scintillator Material*, IEEE Trans. Nucl. Sci. Vol. 51, No. 4, pp. 1672-1676, August 2004.
- 5 D. Cohen, *NORM Characterization of ASP and Multichannel PVT Data*, Sandia Report, SAND2009-8056, March 2010.
- 6 F. Usama, G. Piatetsky-Shapiro, and P. Smyth, *From Data Mining to Knowledge Discovery in Databases*. AI Magazine, Vol. 17, No 2, pp 37-54 1966.
- 7 I.T.Jolloffe, *Principal Component Analysis*, 2<sup>nd</sup> Edition, 2002, Springer-Verlag, New York, Inc.
- 8 C. Fraley, and A.E. Raftery, *MCLUST: Software for Model-Based Cluster Analysis*, Journal of Classification, Vol. 16, pp 297-306, 1999.
- 9 *Handbook of Multisensor Data Fusion*, D.L. Hall and J. Llinas , CRC Press, 2001



This page intentionally left blank

Appendix A: ROC Curves

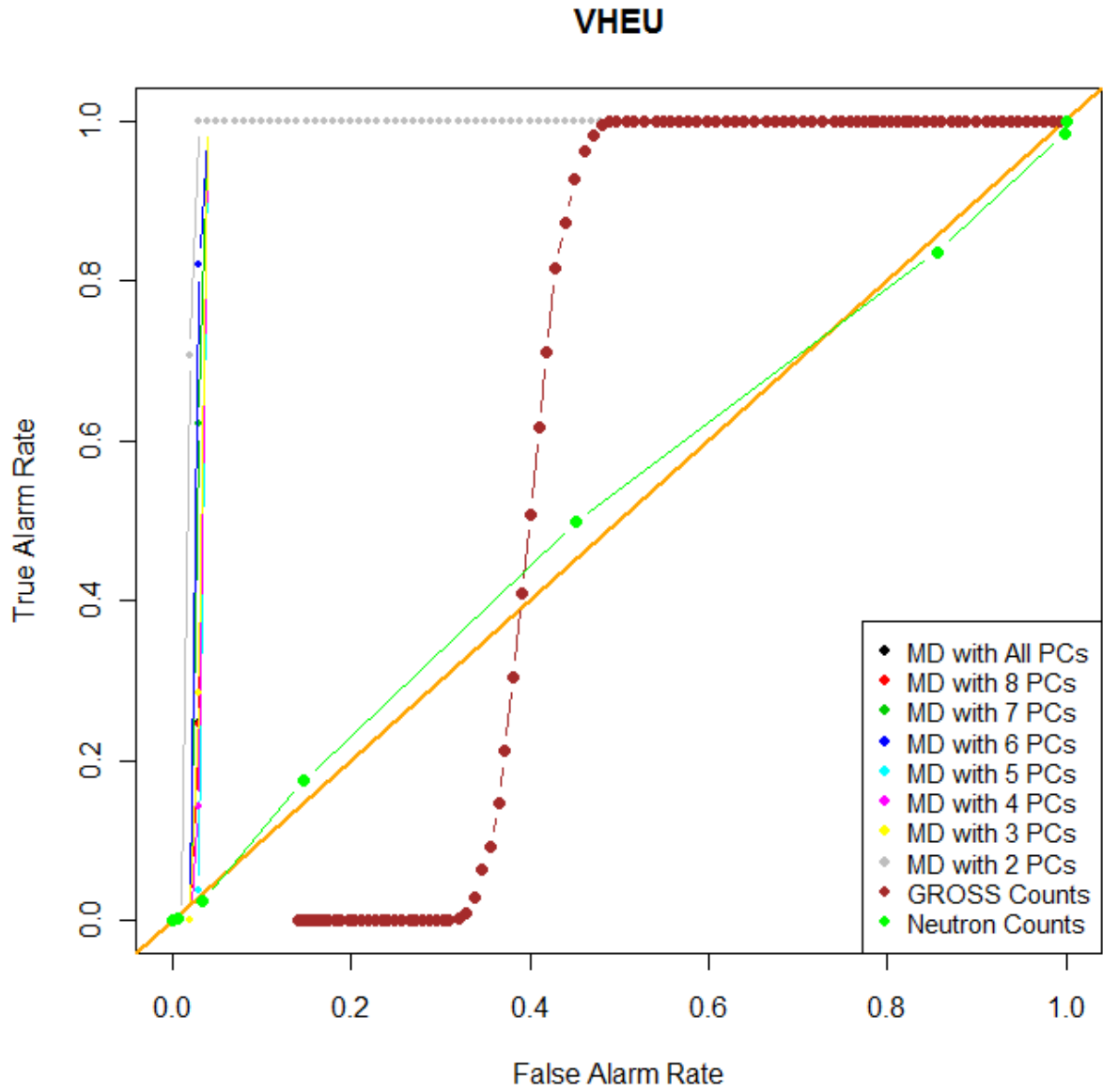
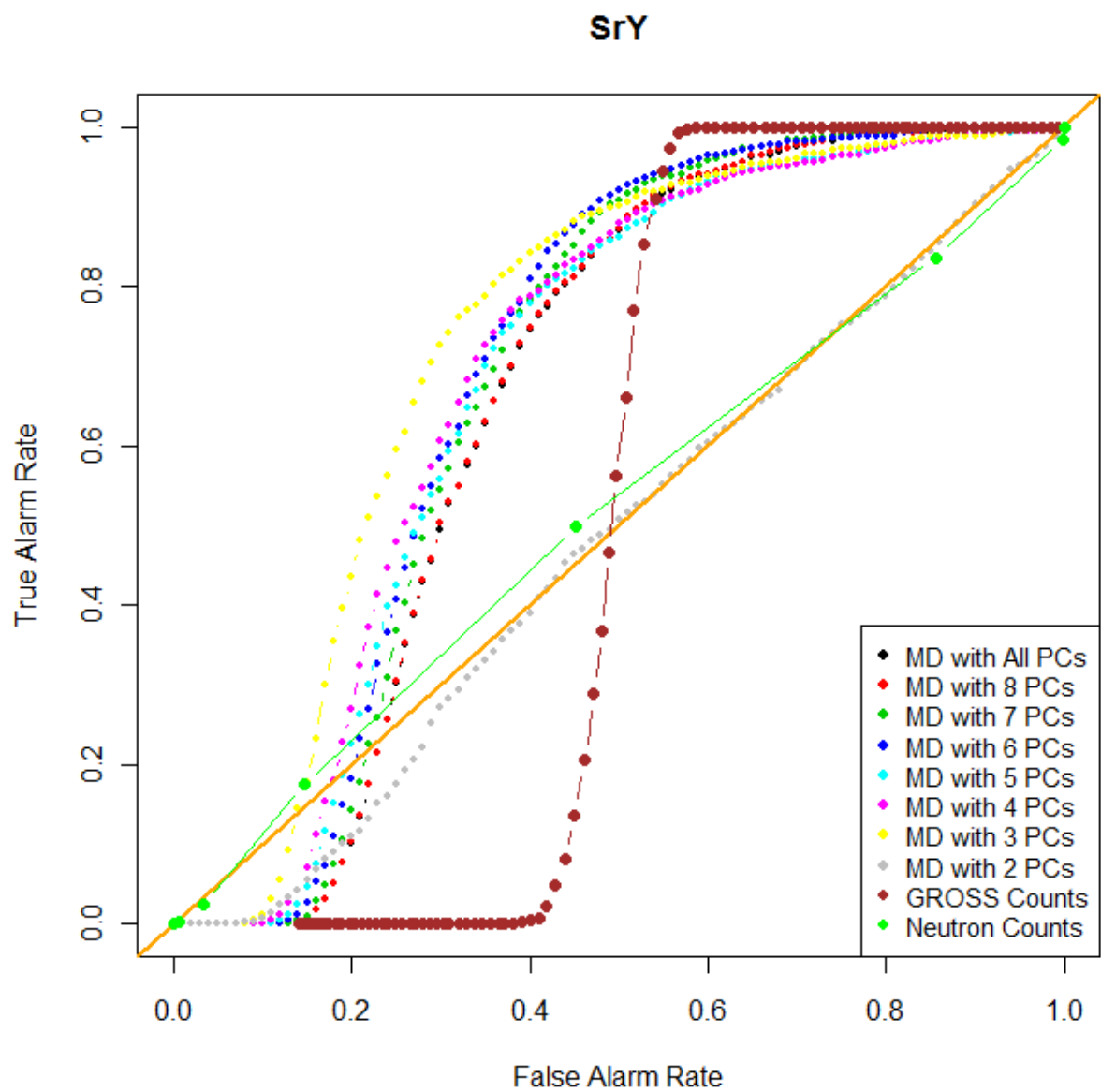
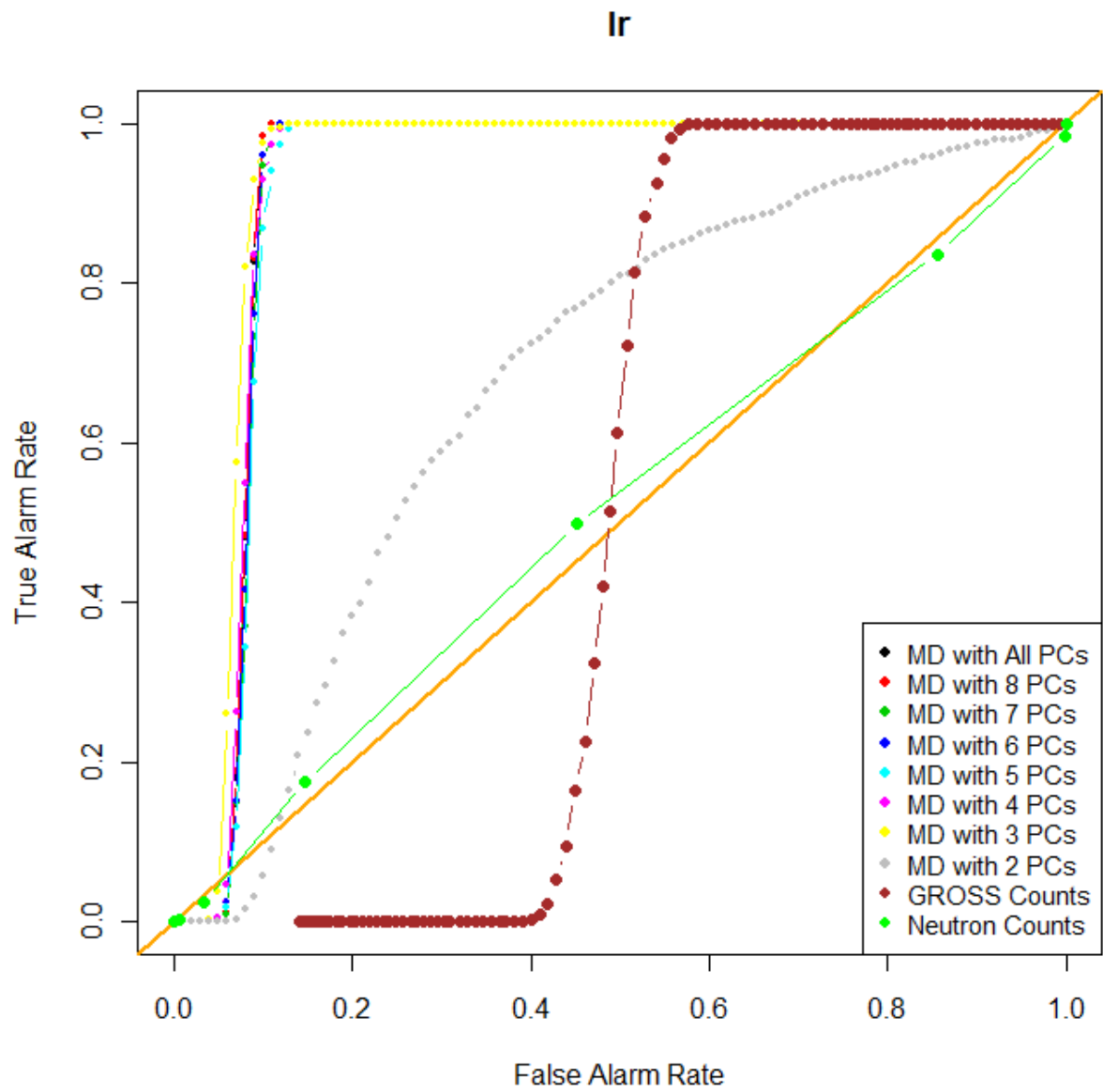


Figure 21 Calculated ROCs for Very High Enriched Uranium (VHEU).



**Figure 22** Calculated ROCs for  $^{90}\text{SrY}$ .



**Figure 23** Calculated ROCs for  $^{192}\text{Ir}$ .

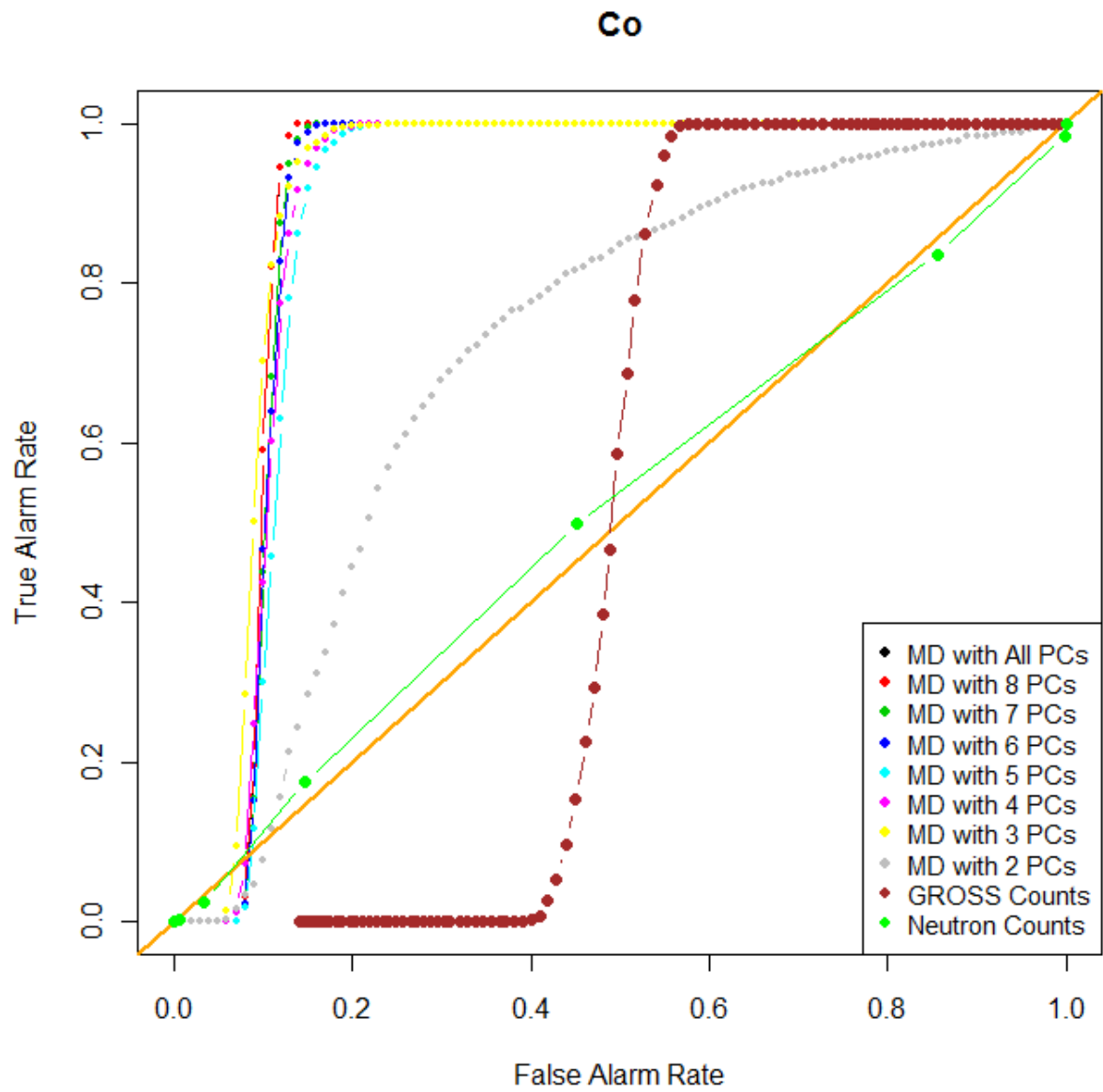


**Figure 24** Calculated ROCs for  $^{60}\text{Co}$ .

This page intentionally left blank

## DISTRIBUTION

1 MS9004 W.P. Ballard 8100  
1 MS9104 W.R. Bolton 8123  
1MS 1377 M. E. Ekman 6813  
1 MS9402 J.E.M. Goldsmith 8131  
1 MS9402 K.L. Hertz 8131  
1 MS9406 N.R. Hilton 8131  
1 MS9104 C.L. Kunz 3131  
1 MS9003 J.C. Reinhardt 8112  
1MS 1379 W. G. Rhodes 6810  
1 MS9104 I.R. Shokair 8123  
1 MS9104 J.R. Spingarn 8131  
1 MS0899 Technical Library 4536  
1MS 9406 C. R. Tewell 8132  
5 MS9406 W. Mengesha 8132  
1MS 1377 E. K. Webb 6814

This page intentionally left blank



